Zeitschrift: IABSE reports = Rapports AIPC = IVBH Berichte
Band: 74 (1996)

Artikel: Ductility requirements of a bridge pier subject to impact
Autor: Cartapati, Enzo
DOI: https://doi.org/10.5169/seals-56105

DUCTILITY REQUIREMENTS OF A BRIDGE PIER SUBJECT TO IMPACT

Enzo CARTAPATI
Senior Researcher
Structural and Geotechn.
Engineering Dept.
University "La Sapienza"
Rome, ITALY

Enzo Cartapati, born in 1946, got his civil engineering degree in 1971 at the University "La Sapienza", Rome, Italy. He has been researcher and encharged professor of Strength of Materials and Construction Technics at the same University.

Summary

The behaviour of a beam, fixed at its ends and axially stressed, subject to the impact of a mass at a given speed is considered. The scope of the paper is to stress the role of ductility in structural elements subject to the impact of deviating vehicles as, e.g., the piers of an overbridge. The behaviour of the pier has been studied through three or four successive phases, taking into account the shear, flexural and axial ultimate stresses. The displacement of impact section is determined as well as the maximum strain at plastic hinges.

1. Introduction

1.1 Foreword

Within a research program on the behaviour of fiber-reinforced concrete structural elements, carried out at the Department of Structural and Geotechnical Engineering of the Rome University "La Sapienza", mono- and bi-dimensional elements subject to repeated dynamic loads and impact have been considered. Experimental tests have been performed on plain and f.r. concrete slabs subject to impact, and on plain and f.r. concrete beams subject to static loads in order to characterize the behaviour of f.r. concrete with respect to plain concrete [1,2]. The present paper follows a recent study [3] on the theoretical aspects of the case of a beam fixed, hinged or simply supported at its ends subject to heavy impact loads. The aim is to underline the ductility requirements of such structures, that, for usual design static equivalent loads, undertake values much beyond those normally accepted for statically loaded structures.

The study of effects of impulsive actions requires the knowledge of physical and mechanical behaviour of materials beyond the elastic field; the structure is studied in the non-linear field of large displacement taking into account the interaction among shear, bending moment and axial stress at ultimate state.

1.2 The materials

The behaviour of materials under impulsive loading beyond elastic limit is very complex.

It depends on several parameters as loading rate, strain rate, instant temperature and steel hardening. Such parameters sometimes are also intercorrelated. Several laws based on theoretical or experimental studies have been proposed for impact loading problems [4,5].

The use of such expressions makes very complex the detailed representation of the behaviour of a structure subject to impact loads. Therefore the influence of the above said parameters is often neglected and rigid-plastic or elasto-plastic laws are considered. Taking into account that, due to the large displacements occurring, the elastically dissipated energy results to be absolutely negligible with respect to the energy dissipated in plastic field, the use of a rigid-plastic model appears quite acceptable and allows a great simplification for the study.

1.3 Structural behaviour and interaction laws

The behaviour of a structure subject to impact loads is characterized by its response in terms of stress distribution and strain development. The collapse mechanism and the variable plasticized sections must be found, depending on the structure shape, load type and materials behaviour. The main aspects to be considered are: the dynamic loads much greater than the static ultimate ones and the large displacements undertaken by the structure. In the first case shear deformations may become not negligible [6,7], in the second one large axial stresses may arise. It turns necessary the account of plastic interaction among bending moment, axial stress and shear stress, that is, the assumption of a suitable plasticization law [8].

Several proposal are at hand in reference [9,10], mainly for steel sections, based on theoretical and experimental studies and related to section and structural shape. For a general steel section or for a reinforced concrete section the following expression has been assumed in [3]:

$$f = \left[\left|\frac{M}{M^*}\right| + \left(\frac{N-N^*}{N_0-N^*}\right)^2 - 1\right]\left(\left|\frac{Q}{Q_0}\right| - 1\right) = 0 \qquad (1)$$

in that N_0 and Q_0 are the ultimate values of tensile stress and shear; M^* is the maximum ultimate bending moment of the section that acts together with the axial stress N^*. For a r.c. section equation (1) approximates with a parabole arch the ductile plastic interaction curve of the section (Fig. 1):

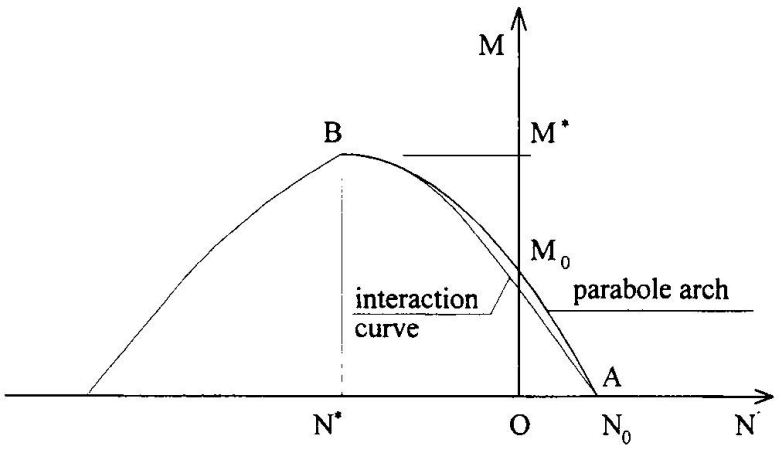

Fig. 1. Interaction curve of reinforced concrete sections.

1.4 The local missile-structure interaction

A further uncertainty contribution, besides those already mentioned, comes from the unknown part of the striking mass energy that is dissipated at impact under damping, friction, sound waves and, mainly, missile deformation. The last contribution is particularly important in the case of impact of deviating vehicles against structures placed close to carriageways. In such case data from experimental tests are quite necessary. In the following it is assumed that the kinetic energy transmitted by the missile to the structure is net from local dissipation and missile deformation. Therefore the impact speed v_0 shall be considered as a reduced speed in order to take into account such dissipated energy. However normatives and constructive recommendations usually propose values of impact forces of deviating vehicles specifying that the whole kinetic energy must be transferred to the impacted structure.

2. Beam dynamic equilibrium

2.1 Assumptions

The development of the structure collapse mechanism is analyzed taking into account the interaction among bending moment, shear and axial stress accordingly with plasticization law (1). In order to reduce the complexity of the problem, the material behaviour is assumed as rigid-plastic and the effect of strain rate and impulse duration is neglected. The analytical results are summarized from [3] and are based on the studies of T. Nonaka [10], but have been extended to different beam end conditions and to a more generic plasticization surface.

2.2 The beam with fixed ends

In this paper, due to synthesis reasons, only the results relative to a beam with fixed ends are reported, allowing for an extension, as limit case, for a hinged beam. The beam, according to the scheme in fig. 2, is impacted at midspan section by a mass m_0 having v_0 velocity.

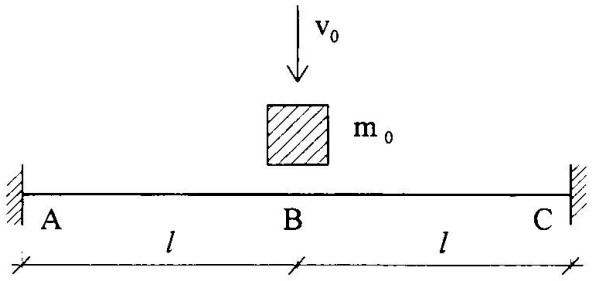

Fig. 2. Scheme of the clamped beam subject to impact.

Referring to above figure: - m is the mass per unit length of the beam; - M_{01} and $M_{02} = M_{01}/K$ the ultimate plastic moments of sections B and C rispectively (with N = 0); - N_{01} and N_{02} the maximum tensile stresses that brings sections B and C to plasticization; - Q_0 the ultimate plastic shear of section B.

2.2.1 First phase

In the first phase, following immediately the impact, the beam, close to the impact area, is subject to a strong shear stress such as to reach the ultimate shear strength and to force the stroken part of the beam to slide with respect to the remaining parts. The half beam limited by the stroken section and the restrained end is subject to the ultimate shear at midspan and to the inertial forces. It begins to rotate producing a plastic hinge at midspan and at its fixed end. The hypothesis is assumed that another plastic hinge takes place at an intermediate position, where inertial forces equilibrate the ultimate shear acting at midspan (Fig. 3).

By means of the impulse theorem and the dynamic equilibrium of the two parts of the half beam, it is possible to determine the end of the relative sliding between the stroken part of the beam and the remaining parts. The speed and the displacement of the stroken part at such instant are determined. Being the displacements very small in this phase, the contribution of axial force is neglected. Assuming $N \cong 0$, it results $M_C \cong M_{02}$ and $M_B \cong M_{01}$.

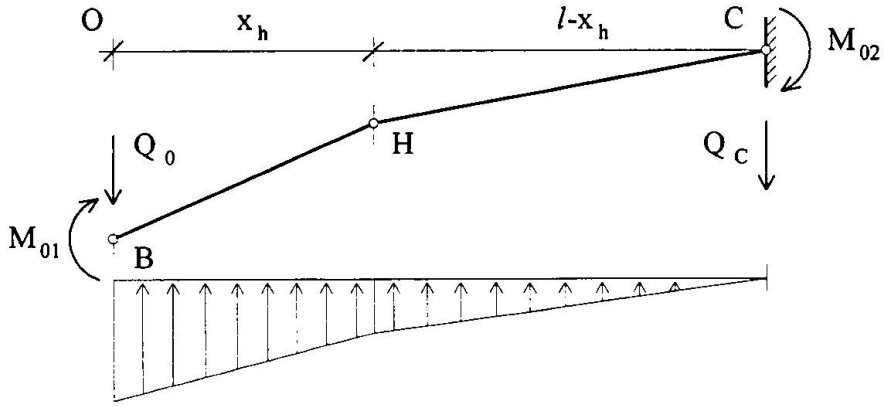

Fig. 3. Scheme of the impacted beam during first phase.

By means of the impulse theorem applied to the striking mass, the speed of the mass is:

$$\dot{y}_0 = \frac{I}{m_0} - \frac{2Q_0 t}{m_0} \tag{2}$$

If $\dot{y}_B$ and $\dot{y}_H$ are the speeds of points B and H, the theorem of the impulse for the part BH gives:

$$Q_0 t = \int_0^{x_h} \left[\dot{y}_B + \frac{\dot{y}_H - \dot{y}_B}{x_h} x \right] m \, dx \tag{3}$$

From the theorem of angular momentum with respect to O, it results:

$$\int_0^{x_h} \left[\dot{y}_B + \frac{\dot{y}_H - \dot{y}_B}{x_h} x \right] x \, m \, dx = 2 M_{01} t \tag{4}$$

Applying the same theorem to part HC with respect to point C, considering x_h costant versus time, it follows:

$$\int_{x_h}^{l} \dot{y}_H \frac{l-x}{l-x_h}(l-x)m\,dx = (M_{01}-M_{02})\,t \qquad (5)$$

From equations (3), (4) and (5) the expressions of $\dot{y}_B$, $\dot{y}_H$ and x_h can be obtained.
The first phase ends when the relative sliding between the stroken part and the remaining part stops; that is if $\dot{y}_B = \dot{y}_0$. From such condition, it results (2):

$$t^* = \frac{I/m_0}{\alpha_1 + 2Q_0/m_0} \qquad (6) \qquad \text{with } \alpha_1 = \frac{2Q_0}{mx_h} - \frac{3\Delta M_0}{m(l-x_h)^2}$$

Equation (6) gives the speed and displacement of midspan section at end of the first phase:

$$\dot{y}_B^* = \alpha_1 t^* \quad ; \quad y_B^* = \frac{\alpha_1}{2} t^{*2}$$

and $\dot{y}_H^* = \alpha_2 t^*$ with $\alpha_2 = \dfrac{3\Delta M_0}{m(l-x_h)^2}$

At the end of this phase it is possible to check the hypothesis of the formation of the intermediate plastic hinge: it happens if the angular speed $\dot{y}_B/l$ is greater than $\dot{y}_H/(l-x_h)$, that is:

$$\frac{\alpha_1(l-x_h)}{\alpha_2 l} > 1 \qquad (7)$$

If inequality (7) is not true, only the plastic hinges in B and C take place; the theorems of impulse and angular momentum applied to the whole half beam give the following expressions:

$$(Q_0 - q)t = \frac{\dot{y}_B m l}{2} \quad ; \quad \frac{m\dot{y}_B l^2}{6} = \left(M_{01} + \frac{M_{01}}{K} - ql\right)t$$

from which we can obtain:

$$\dot{y}_B = \alpha_3 t \qquad \text{with} \qquad \alpha_3 = 3\frac{Q_0 l - M_{01}(1+1/K)}{ml^2}$$

In analogy with the preceeding case, it results:

$$t^* = \frac{I/m_0}{\alpha_3 + 2Q_0/m_0} \quad ; \quad \dot{y}_B^* = \alpha_3 t^* \quad ; \quad y_B^* = \frac{\alpha_3}{2} t^{*2}$$

2.2.2 Second phase

In the second phase, that is present only if the intermediate plastic hinge takes place, such hinge moves rapidly towards the restrained end of the beam, because of the reduced shear force and the increase of axial force effect. This phase develops very quickly and can be examined by means of the conservation of kinetic energy through the end of phase one and the

end of phase two. The speed and the displacement of midspan section at the end of this phase are determined:

$$E = \frac{m(l-x_h)\dot{y}_H^{*2}}{6} + \frac{1}{4}m_0\dot{y}_B^{*2} + \frac{1}{2}m\int_0^{x_h}\left(\dot{y}_B^{*} + \frac{\dot{y}_H^{*} - \dot{y}_B^{*}}{x_h}x\right)^2 dx = \frac{1}{4}m_0\dot{y}_x^2 + \frac{1}{6}ml\dot{y}_x^2$$

$$y_x = \sqrt{\frac{m\dot{y}_H^{*}\left(\dot{y}_H^{*}l + \dot{y}_B^{*}x_h\right) + \dot{y}_B^{*2}\left(\frac{3}{2}m_0 + mx_h\right)}{\frac{3}{2}m_0 + ml}}$$

2.2.3 Third phase

The third phase is the most important one, due to the presence of axial stress which gives its contribution to dissipate, together with the plastic hinges, the residual kinetic energy. The axial force must be considered in this phase because the displacements become not negligible; therefore the interaction N - M will be taken into account..

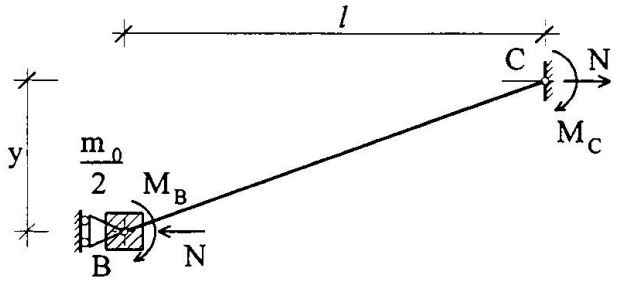

Fig. 4. Scheme of the impacted beam during third phase.

At plastic hinges B and C, whose equivalent lengths can be assumed as d_1 and d_2, the strain rate vector has components:

$$\dot{\varepsilon}_1,\ \dot{K}_1,\ 0 \qquad \text{in B}$$
$$\dot{\varepsilon}_2,\ \dot{K}_2,\ 0 \qquad \text{in C}$$

being ε and K the axial strain and the curvature. The axial strain rate of the beam is:

$$\dot{\Delta l} = \frac{\partial(l'-l)}{\partial t} = \frac{\partial}{\partial t}\left(\sqrt{y^2+l^2}\right) = \frac{y\dot{y}}{\sqrt{y^2+l^2}} \cong \frac{y\dot{y}}{l}$$

If the axial strain is localized in B and C according to the quantities s and 1-s, it follows:

$$\dot{\varepsilon}_1 = \frac{sy\dot{y}}{d_1 l} \quad ; \quad \dot{\varepsilon}_2 = \frac{(1-s)y\dot{y}}{d_2 l} \quad ; \quad \dot{K}_1 = \frac{\dot{y}}{d_1 l} \quad ; \quad \dot{K}_2 = \frac{\dot{y}}{d_2 l}$$

Furthermore the strain rate vector is constrained to be tangent to the yield surface; therefore:

$$\frac{\dot{\varepsilon}}{\dot{K}} = \frac{\partial f}{\partial N}\Big/\frac{\partial f}{\partial M} = \frac{2(N-N^{*})}{(N_0-N^{*})^2}M^{*}$$

From the preceeding expressions it follows:

$$N = \frac{(N_{01} - N_1^*)^2}{2M_1^*} sy \quad ; \quad N = \frac{(N_{02} - N_2^*)^2}{2M_2^*}(1-s)y \tag{8}$$

Those expressions allow the determination of s; being:

$$K^* = \frac{M_1^*}{M_2^*} \quad \text{and} \quad H = \frac{(N_{02} - N_2^*)^2}{(N_{01} - N_1^*)^2} \quad , \quad s = \frac{K^*H}{1+K^*H} \tag{9}$$

Referring to fig. 4, by means of the dynamic equilibrium of moments acting on the halfbeam with respect to point C, it results:

$$\frac{1}{2} l m_0 \ddot{y} + \int_0^l \frac{\ddot{y}}{l} x^2 m \, dx + M_B + M_C + Ny = 0 \tag{10}$$

Using the interaction law (1), substituting the expression of N (8) and s (9); multiplying by $\dot{y}$, integrating and introducing the following constants:

$$\alpha = \frac{l m_0}{4M_1^*} + \frac{l^2 m}{6M_1^*} \quad ; \quad \beta = \frac{K^*(N_{02} - N_2^*)^2}{12M_1^{*2}(1+K^*H)}$$

$$\gamma = \frac{N_1^* K^* H + N_2^*}{2M_1^*(1+K^*H)} \quad ; \quad \delta = \left(1 + \frac{1}{K^*}\right) - \frac{N_1^{*2} K^* H + N_2^{*2}}{K^*(N_{02} - N_2^*)^2}$$

equation (10) becomes:

$$\alpha \dot{y}^2 + \beta y^3 + \gamma y^2 + \delta y = \text{cost}$$

The motion stops when $\dot{y} = 0$; it results then:

$$\beta y_u^3 + \gamma y_u^2 + \delta y_u = \alpha \dot{y}^{*2} + \beta y^{*3} + \gamma y^{*2} + \delta y^*$$

where $\dot{y}^*$ and y^* are known from preceeding phases. This equation allows to obtain the final displacement y_u of midspan section B.

The value of N from equation (8) must be compared with the maximum value at point A of fig. 1, that is with N_{02}. When N reaches such value, it results from (8):

$$y_M = \frac{2N_{02}M_1^*}{s(N_{01} - N_1^*)^2}$$

If y_u is lower than y_M, the motion effectively stops; otherwise, if $y_u > y_M$, N reaches the value of N_{02} and keeps constant. In this case it is necessary to consider a further phase.

2.2.4 Fourth phase

In the fourth phase the axial stress is kept constant at its maximum value and no bending moment is taken into account in the weakest hinge for the dynamic equilibrium. According to

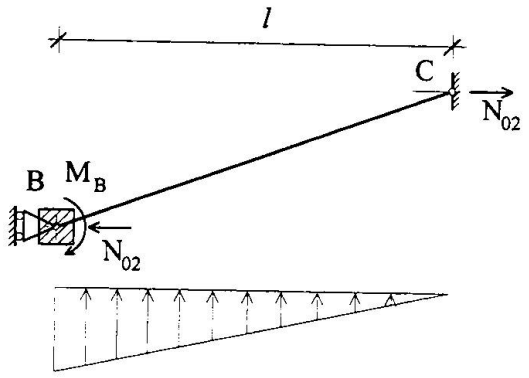

Fig. 5. Scheme of the impacted beam during fourth phase.

the static scheme of fig. 5, equation (10) becomes:

$$2\alpha\,\ddot{y} + \frac{M_B}{M_1^*} + \frac{N_{02}}{M_1^*}\,y = 0$$

Following the same steps as for phase three, for:

$$b = \frac{N_{02}}{2M_1^*} \qquad ; \qquad c = 1 - \left(\frac{N_{02} - N_1^*}{N_{01} - N_1^*}\right)^2$$

it results:

$$by_u^2 + cy_u = \alpha\,\dot{y}_M^2 + by_M^2 + cy_M = \text{cost} - \beta\,y_M^3 - \gamma\,y_M^2 - \delta\,y_M + by_M^2 + cy_M$$

from which it is possible to obtain the final displacement y_u of midspan section.

3. The case of an overbridge pier

The results just obtained have been applied to the case of an overbridge pier subject to the impact of a deviating truck. The reinforced concrete pier of an overbridge is 8.0 m high and the deviating truck, coming from a road on embankment, strikes the pier at halfheight at the velocity of 50 km/h. The mass of the truck is 30000 kg (see [11], par 4.3, table 4.3.1, urban area). The static equivalent impact load is 2000 KN. Static calculations and ultimate moments and forces evaluation have been carried out with reference to Eurocode 2 [12]. Two different square sections have been considered: 1.00x1.00 m and 1.20x1.20 m. Variable percentages of bending reinforcement have been taken into account and variable strength ratios between midspan and fixed end sections, in order to study different restraint condition from the perfectly clamped beam with constant strength to the end-hinged beam. For each section two different shear reinforcements have been considered: the lower reinforcement designed with reference to the static equivalent impact force, the higher nearly twice the first one. The results of dynamic calculations of displacements for impact velocity of 10 m/s have been reported in figures from 6 to 9. In the diagrams the plastic strains of bending reinforcement are represented versus reinforcement percentage for different ultimate moment ratios of midspan and fixed end sections. Plastic strain of bending reinforcement has been calculated from final displacement of midspan section considering the localized rotations at plastic

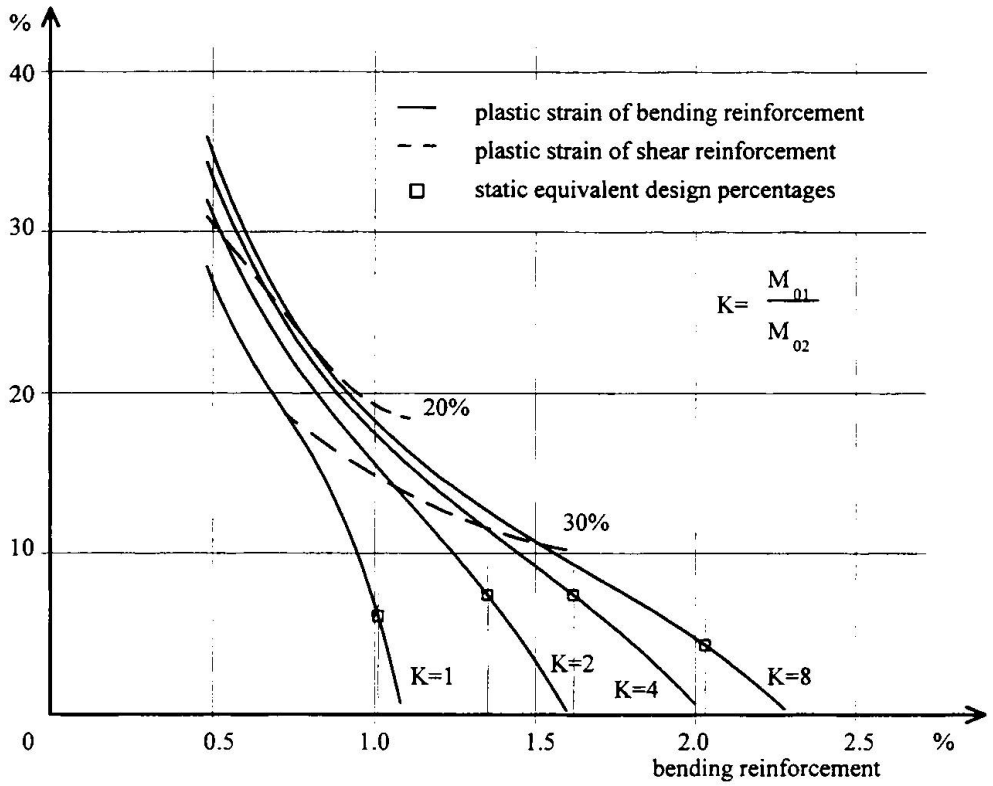

Fig. 6. Bending and shear reinforcement strains.
Section 1.00x1.00 m, stirrups 4ϕ 12mm/250mm.

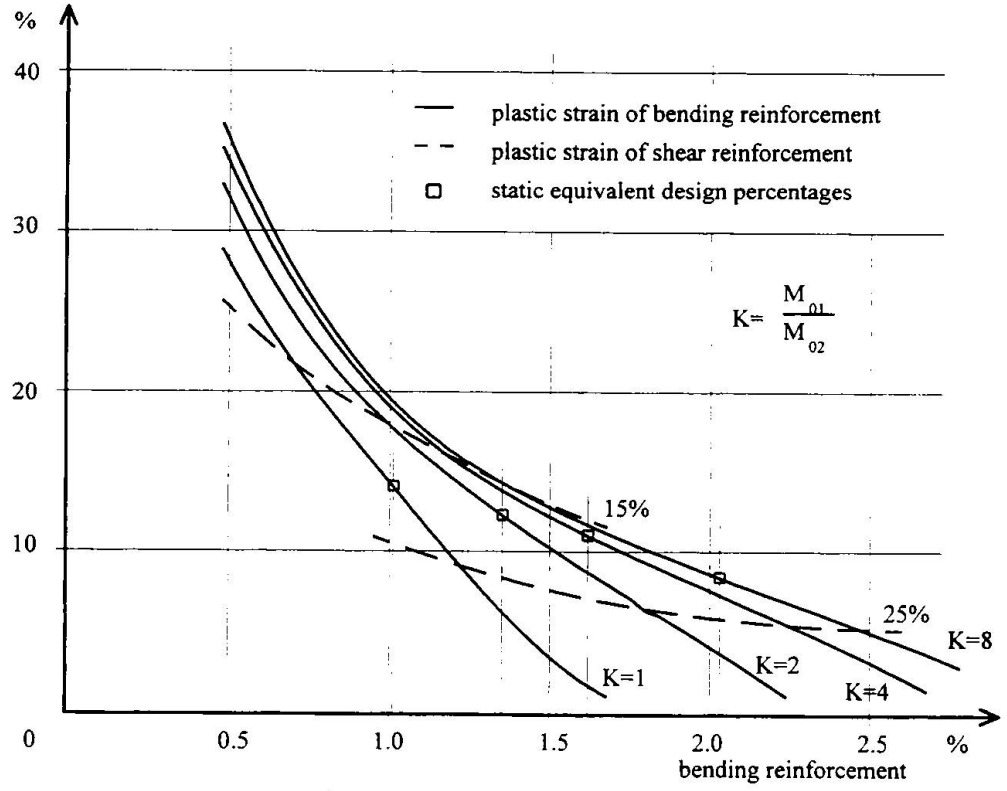

Fig. 7. Bending and shear reinforcement strains.
Section 1.00x1.00 m, stirrups 4ϕ 14mm/200mm.

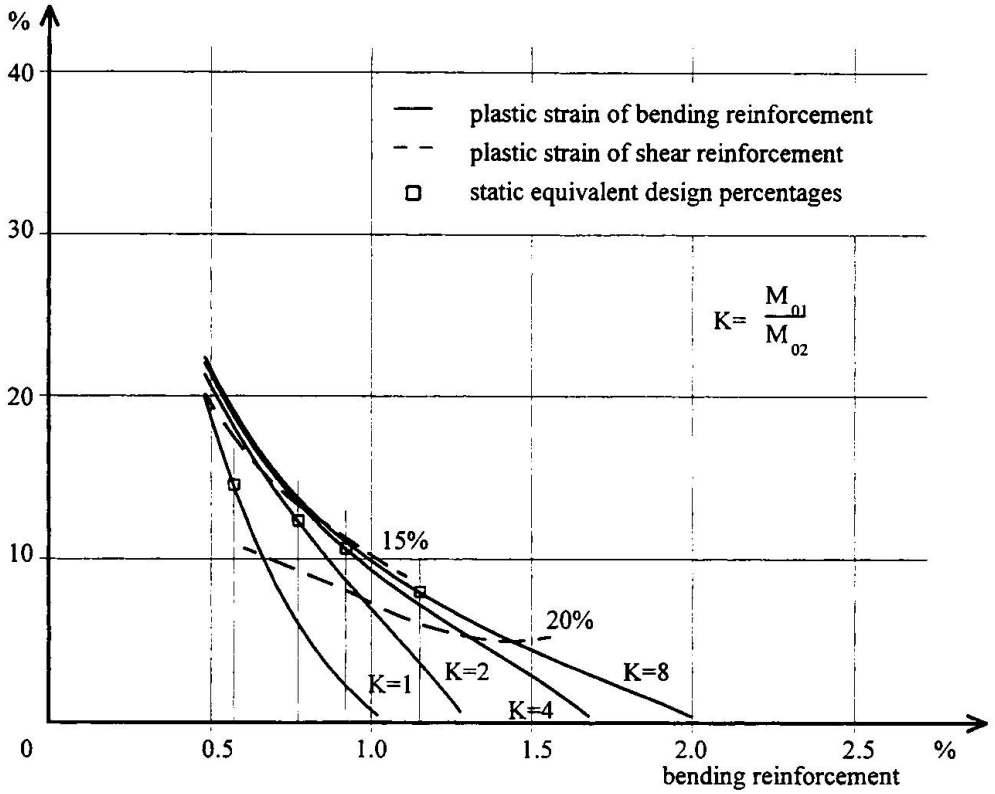

Fig. 8. Bending and shear reinforcement strains.
Section 1.20x1.20 m, stirrups 4ϕ 12mm/200mm.

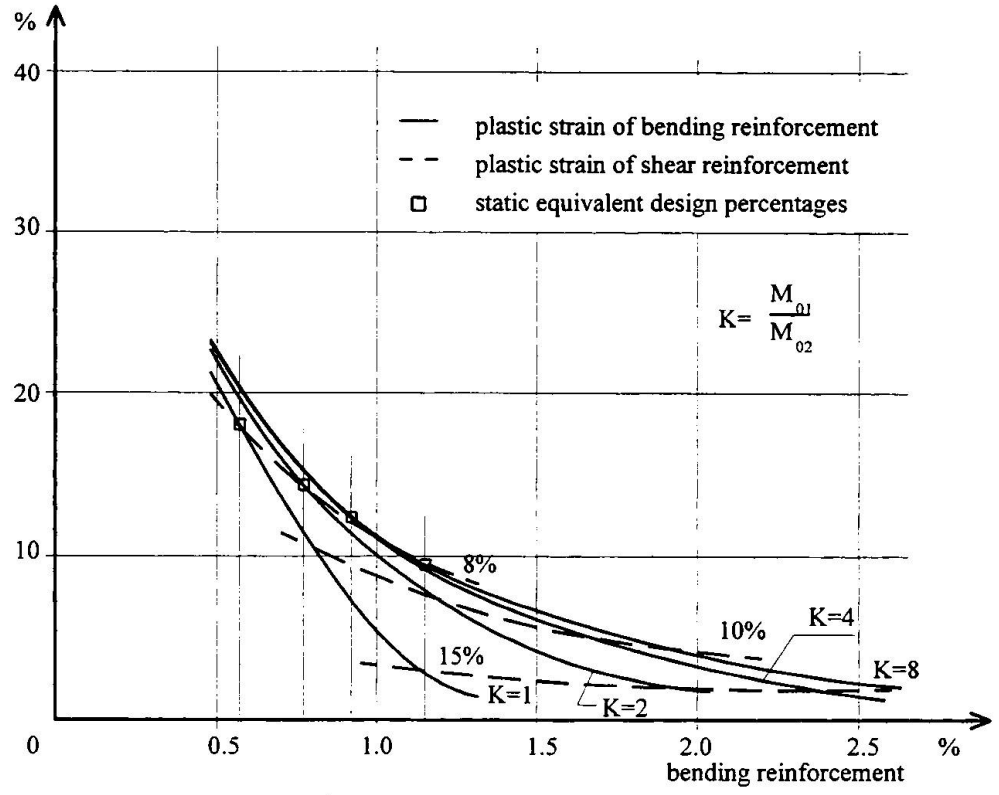

Fig. 9. Bending and shear reinforcement strains.
Section 1.20x1.20 m, stirrups 6ϕ 14mm/200mm.

hinges and the length of strained reinforcement as twice the equivalent length of plastic hinge [13], that is about 1.2 times the effective depth of cross section. Diagrams are given also for the plastic strain of shear reinforcement, that varies with the bending reinforcement percentage. Stirrups strain, considered constant along the full depth of the section, has been calculated from the relative displacement due to the sliding that occurs during the first phase.

The mechanical characteristics of materials are:
- characteristic strength of concrete: $f_{ck} = 25$ N/mm^2
- characteristic yield strength of reinforcing steel: $f_{yk} = 440$ N/mm^2

4. Concluding remarks

Although the data reported in fig. 6-9 refer to a particular case, it seems very clear that the results of dynamic calculations leed to values of reinforcement strain much greater than static calculations. Moreover close to impact section the ultimate shear strength is reached immediately after impact and causes a remarkable localized sliding of the part directly in contact with the missile with respect to the remaining part of the beam, until relative speed vanishes. Such localized sliding produces very high strain in shear reinforcement. On the other side, increasing shear strength reduces inversely shear reinforcement strain but increases bending reinforcement strain, because less kinetic energy is dissipated at impact zone and plastic hinges undergo an increase of localized rotation.

Furthermore it must be noted that dynamic calculations have been carried out for a reduced impact velocity (10 m/s instead of 13.89 m/s = 50 km/h) in contrast respect to the application rule given in [11] at par. 4.2, where it is suggested that " all available energy of the colliding object is fully transferred into elastic or plastic deformation energy of the structure".

With reference to restraints conditions it seems more favourable the choice of a hinged beam with a higher bending reinforcement percentage, because for the same bending reinforcement strain the shear reinforcement strain is reduced. On the contrary, small increases of bending reinforcement in fixed end beam with uniform strength leed quickly to a condition in which the greater part of kinetic energy of the impacting body is dissipated by shear reinforcement with too high strain levels.

Finally, it seems necessary that designing with respect to an accidental action like impact be performed by means of a dynamic analysis of the structure; otherwise the analysis for a static equivalent load model must be accompanied by specific recommendations that take into account the inertia effects in order to limit reinforcement strains.

The account of strain rate and strain hardening effects reduces the strains evaluated and reported in above diagrams, but the reduction is small compared with the absolute value of computed strains. Further investigation on the topic is in program. Anyway introducing iterative procedures at intermediate stages of preceding calculations may improve the reliability of results, but doesn't change the mutual interdependence of main parameters.

5. References

1. Calamani S., Cartapati E., Materazzi A.L.: "Impact behaviour of polypropylene-fiber-reinforced concrete plates", Eight european Conference on Fracture, Fracture Behaviour and Design of Materials and Structures, Torino, 1-5 October 1990, pag. 755-760.

2. Radogna E.F., Cartapati E., Materazzi A.L.: "Piastre di conglomerato cementizio rinforzato con fibre "morbide" sottoposte ad azioni impulsive: problemi di modellazione e verifiche sperimentali", Giornate A.I.C.A.P. '91, Spoleto, 16-18 may 1991, pag. 409-424.

3. Cartapati E.: "Indagine teorico-sperimentale sull'effetto di azioni impulsive su elementi strutturali lineari", Studi e Ricerche, Dipartimento di Ingegneria Strutturale e Geotecnica, Università di Roma "La Sapienza", gennaio 1996.

4. Jones N.: "Influence of strain hardening and strain rate sensitivity on the permanent deformation of beams", International Journal of Mechanical Science, Vol. 9, 1967.

5. CEN: Bulletin d'information n°187: "Concrete structures under impact and impulsive loading", August 1988.

6. Bleich H.H., Shaw R.: "Dominance of shear stresses in early stages of impulsive motion of beams", Journal of Applied Mechanics, Vol. 27, March 1960.

7. Karunes B., Onat E.T.: "On the effect of shear on plastic deformation of beams under transverse impact loading", Journal of Applied Mechanics, Vol. 27, March 1960.

8. Neal B.G.: "The effect of shear and normal forces on the fully plastic moment of a beam of a rectangular cross section", Transactions ASME, Vol. 83, Series E, June 1961, pag.269-274.

9. Hodge P.G.: "Interaction curves for shear and bending of plastic beams", Transactions ASME, Vol. 79, September 1957, pag. 453-456.

10. Nonaka T.: "Some interaction effects in problem of plastic beam dynamics - Parts 1,2,3", Journal of Applied Mechanics, Vol. 34, September 1967, pag.623-643.

11. CEN: EUROCODE 1: Basis of design and actions on structures. Part 2-7: Accidental actions. Draft, June 1995.

12. CEN: EUROCODE 2: Design of concrete structures. Part 1: General rules and rules for buildings. Final Draft, 31 october 1990.

13. Park R., Pauley T.: "Reinforced Concrete Structures", John Wiley & Sons, New York, 1975.